Polarized Raman Study of Single-Wall Semiconducting Carbon Nanotubes

A. Jorio, G. Dresselhaus, and M. S. Dresselhaus
Massachusetts Institute of Technology, Cambridge, Massachusetts 02139-4307

M. Souza, M. S. S. Dantas, and M. A. Pimenta
Departamento de Física, Universidade Federal de Minas Gerais, Belo Horizonte–MG, 30123-970 Brazil

A. M. Rao*
Center for Applied Energy Research, Department of Physics and Astronomy, University of Kentucky, Lexington, Kentucky 40506

R. Saito
Department of Electronics-Engineering, University of Electro-Communications, Tokyo, 182-8585 Japan

C. Liu and H. M. Cheng
Institute of Metal Research, Chinese Academy of Sciences, Shenyang 110015, China
(Received 5 April 2000)

Polarized Raman spectra were obtained from a rope of aligned semiconducting single-wall nanotubes (SWNTs) in the vicinity of the D band and the G band. Based on group theory analysis and related theoretical predictions, the G-band profile was deconvolved into four intrinsic SWNT components with the following symmetry assignments: 1549 cm^{-1} $[E_2(E_{2g})]$, 1567 cm^{-1} $[A(A_{1g}) + E_1(E_{1g})]$, 1590 cm^{-1} $[A(A_{1g}) + E_1(E_{1g})]$ and 1607 cm^{-1} $[E_2(E_{2g})]$. The frequency shifts of the tangential G modes from the $2D$ graphitelike E_{2g_2} frequency are discussed in terms of the nanotube geometry.

PACS numbers: 78.30.Na, 78.66.Tr

Raman scattering has been extensively used to study the 1D characteristics of (n, m) carbon nanotubes and to characterize their geometric structure [1]. Particular attention has been given to the radial breathing mode (RBM) [1–3] and to the tangential stretching G-band modes [1,2,4]. The properties of the RBM (symmetry and dependence on nanotube geometry) have already been well established [2,3,5]. Because of the folding of the graphite Brillouin zone into the nanotube zone and because of the nanotube curvature, the G band in nanotubes contains several modes with different symmetries. The tangential modes that are Raman active exhibit A, E_1, and E_2 (A_{1g}, E_{1g}, and E_{2g} for symmorphic groups) [1,6,7] symmetries, but very few polarization studies have thus far been carried out [5,8,9] and their symmetry assignments are not yet well established. We recently performed a polarized micro-Raman study on an aligned bundle of multiwalled carbon nanotubes (MWNTs) [8], but MWNTs have relatively large tube diameters, so that the tangential mode frequencies are not sufficiently split to be distinguished in a symmetry analysis of the spectra. The study of single-wall nanotubes (SWNTs), which constitute a more fundamental system, is necessary to obtain a detailed symmetry assignment for the tangential stretching modes in carbon nanotubes. Sun *et al.* [5] performed a preliminary polarized Raman study on SWNTs, but the observed line shape was quite different from previously observed spectra for SWNTs [1,2,4].

We here report a detailed polarized Raman study on a sample of aligned SWNTs in the spectral region of the D band and G band. We analyze the polarized Raman spectra of *semiconducting* nanotubes with regard to the mode symmetry identification. We do not extend this study to the tangential bands of *metallic* SWNTs, because the metallic nanotubes show a $\sim$1540 cm^{-1} Breit-Wigner-Fano feature [10] whose origin is not yet well understood theoretically.

Aligned SWNTs were prepared using a hydrogen and argon electric arc method [11]. The measured sample is composed of a few bundles of SWNTs having very good microscale tube alignment (see lower part of Fig. 1). From TEM and HRSEM observations, the SWNT bundle also shows good nanoscale tube alignment, with a large majority of SWNTs exhibiting a distribution of alignment angles within $\sim$10° (see upper part of Fig. 1). Backscattering Raman spectra were performed at 300 K using a triple-monochromator DILOR XY micro-Raman spectrometer. The 514.5 nm ($E_\ell = 2.41$ eV) laser excitation was used to resonantly select *semiconducting* SWNTs [1,2,4]. The Raman spectrum in the RBM region (see inset to Fig. 2) indicates a broad distribution of tube diameters that are in resonance with the 514.5 nm laser excitation [1–3], in agreement with the previous diameter characterization for this sample [11], where nanotubes with larger diameters ($d_t = 1.85 \pm 0.25$ nm) are dominant, although smaller (down to 1.3 nm) and larger (up to 2.5 nm) diameter tubes can be found in the sample. Polarized Raman spectra in the D and G-band regions were collected from the same spot in the sample (experimental precision ± 1 cm^{-1}). We consider the $\hat{Y}$ direction as the light propagation direction, and the $\hat{Z}$ direction as the nanotube axis direction (see axes in the lower part of Fig. 1). We used (ZZ), (XX), (ZX),

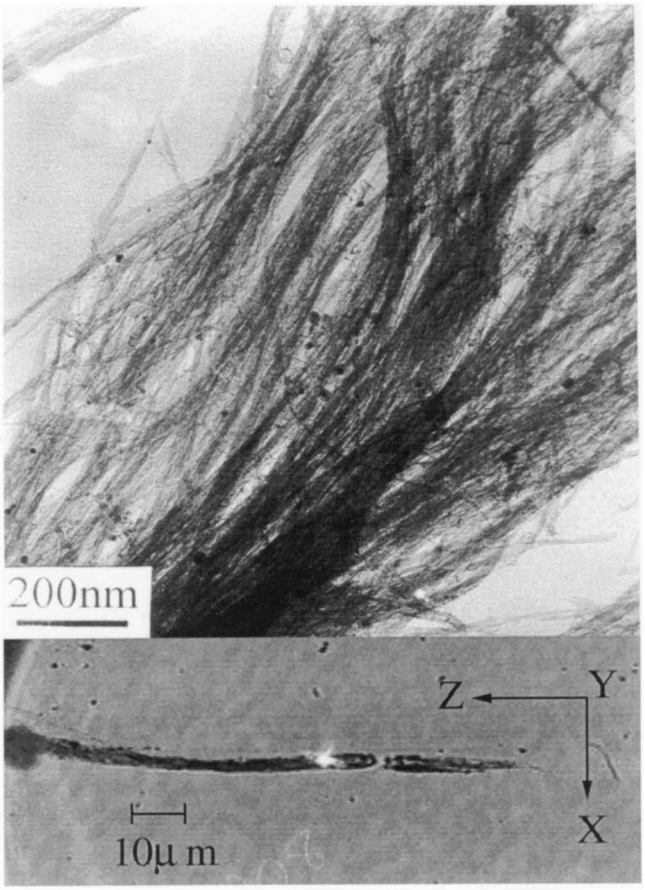

FIG. 1. TEM (upper part) and photo (lower part) images of the rope of SWNT bundles used in the polarized Raman study. The symmetry axes and laser spot (bright area) are indicated.

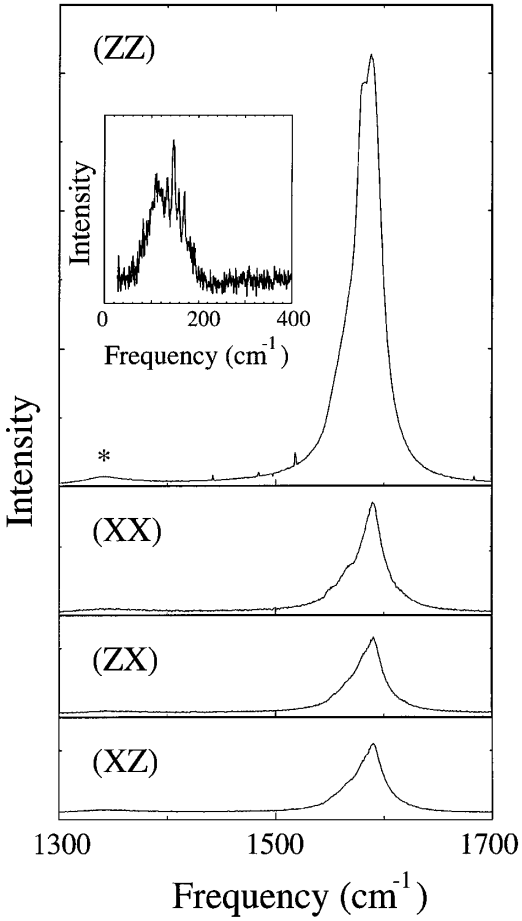

FIG. 2. Raman spectra of an aligned bundle of semiconducting SWNTs in the region of the D band ("$*$") and the G band in various scattering polarizations. The inset shows the (ZZ) polarized Raman spectra of the RBM region. The RBM spectra have practically no intensity in the crossed polarization geometries. We did not use as long an exposure data collection time for the RBM region, as we did for the G-band region, thus explaining the noisy RBM spectrum.

and (XZ) polarization geometries, where the letters indicate the polarization directions of the (incident, scattered) light. Figure 2 shows Raman spectra of the aligned SWNT sample in the region of the D band and of the G band using the four scattering polarization geometries. The intensities of the modes are strongly sensitive to the experimental scattering geometry. The D band appears at 1341 cm^{-1} with very low intensity, but also exhibits a strong polarization dependence, as previously observed in MWNTs [8].

For *semiconducting* SWNTs, a Lorentzian line shape is expected for the various G-band modes. Figure 3 shows a fit of the four polarized G-band Raman spectra in Fig. 2 using five Lorentzians, with frequencies (widths): 1549(12), 1567(30), 1580(10), 1590(20), 1607(33) cm^{-1}. Except for the graphitelike (1580 cm^{-1}) line, the spectra in Fig. 3 show good agreement with previously published results [1,2,4]. The peaks are broader in comparison to previous publications, consistent with the broader range of tube diameters present in this aligned sample [11]. Although the 1580 cm^{-1} peak exhibits a strong polarization dependence, this feature is absent in previously published Raman spectra for semiconducting SWNTs, and its relative intensity, compared with other lines in the spectra, varies from spot to spot on the sample. These results indicate that this line is not an intrinsic feature of semiconducting SWNTs.

Although the presence of nanotube-nanotube interactions may cause some changes in the vibrational behavior of SWNTs in bundles, including symmetry breaking effects, these interactions have been shown not to be important for the G-band Raman spectra of SWNTs under ambient conditions [12], so that the free nanotube symmetries (D_{nh}, D_{nd}, or $C_{N/\Omega}$ [1]) can be used. According to group theory analysis, six modes can be present in the G band of SWNTs: two $A(A_{1g})$, two doubly degenerate $E_1(E_{1g})$, and two doubly degenerate $E_2(E_{2g})$ modes. For each symmetry mode, the atomic vibrations can be along the tube axis direction, or along the circumferential direction. In the zigzag and armchair tubes (symmorphic groups), because of the high symmetry, only three of the six peaks can be seen in a Raman spectrum [6,7,13]. For general chiral tubes (nonsymmorphic groups), the direction of the atomic vibrations is no longer parallel or

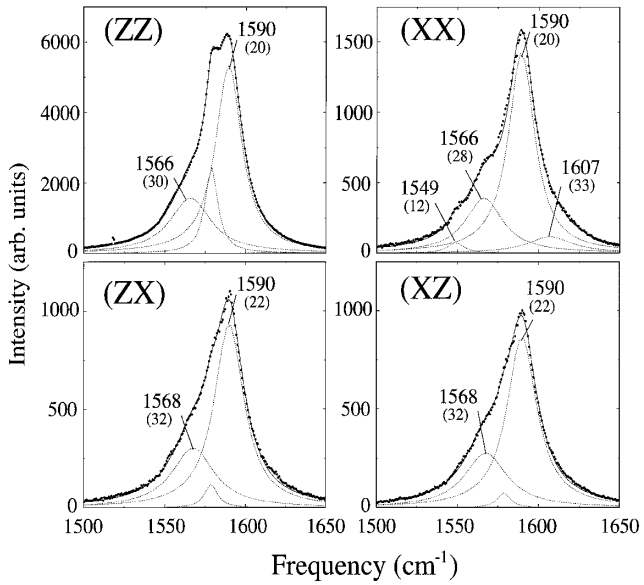

FIG. 3. Lorentzian line shape analysis for the four polarized spectra in Fig. 2. The frequencies (widths) of the observed modes are also displayed. The unlabeled peak (1580 cm^{-1}) is not related to an intrinsic Raman feature of semiconducting SWNTs. When referring to the peaks that appear at 1566 and 1568 cm^{-1} in the text and Table I, we use the average value of 1567 cm^{-1}.

perpendicular to the C-C bonds, but rather depends on the chiral angle, and six peaks can appear in the Raman spectra [6,13]. Considering the scattering geometries of Fig. 2, the totally symmetric $A(A_{1g})$ modes can be observed in the parallel polarized spectra, the $E_1(E_{1g})$ modes can be observed in the cross polarized spectra, and the $E_2(E_{2g})$ modes can be observed only in the (XX) parallel polarized spectra. Saito *et al.* [7] computed the peak intensities for the polarized spectra in a well-oriented (10,10) armchair nanotube. We compare our results with theoretical expectations [7] for an armchair nanotube, since these are the only theoretical polarization results presently available for SWNTs. The calculations were performed within nonresonant theory and neglecting the depolarization effect predicted by Ajiki and Ando [14], and these symmetry results are expected to apply to semiconducting nanotubes also.

Our experimental results show that the highest frequency 1607 cm^{-1} tangential mode appears with low intensity in the (XX) parallel polarized spectra, and is absent in the other polarized spectra (see Fig. 3 and Table I). This result is in agreement with group theory predictions for the $E_2(E_{2g})$ mode. According to theoretical calculations, low intensity is expected for this mode [$I_{A_{1g}(ZZ)}$:$I_{E_{2g}(XX)}$ = 1.00:0.11, taking the A_{1g} intensity in the (ZZ) polarized spectra as a reference] [7]. Although the lowest frequency 1549 cm^{-1} tangential mode exhibits very low intensity in the spectra obtained with the single aligned bundle of SWNTs (see Fig. 3 and Table I), a similar discussion suggests that the 1549 cm^{-1} mode also has $E_2(E_{2g})$ symmetry. The central peaks at 1567 and 1590 cm^{-1} exhibit

TABLE I. Relative intensities of the G-band modes belonging to different irreducible representations (IR) in the polarized Raman spectra of semiconducting SWNTs. For the modes at 1567 and 1590 cm^{-1}, we used their measured intensities in the (ZZ) polarized spectra as a reference, while for the modes at 1549 and 1607 cm^{-1}, we used the (ZZ) intensity of the 1590 cm^{-1} mode as a reference.

ω (cm^{-1})	IR	(ZZ)	(XX)	(ZX)	(XZ)
1549	$E_2(E_{2g})$	0.00	0.01	0.00	0.00
1567	$A(A_{1g}) + E_1(E_{1g})$	1.00	0.23	0.21	0.19
1590	$A(A_{1g}) + E_1(E_{1g})$	1.00	0.26	0.19	0.18
1607	$E_2(E_{2g})$	0.00	0.04	0.00	0.00

an intensity ratio $I_{(ZZ)}$:$I_{(XX)} \sim$ 1.00:0.25 (see Table I). This result was also observed for MWNTs [8], and is in very good agreement with predictions [7] for the A_{1g} mode of a (10,10) nanotube. However, the cross polarized (ZX) and (XZ) spectra also exhibit two central features at 1567 and 1590 cm^{-1}, indicating that these peaks should also be assigned to $E_1(E_{1g})$ symmetry. According to the theory [7] for the θ_1 (angle between the nanotube axis and electric field polarization) angular dependence in a (10,10) nanotube (including averaging over θ_3—the rotation of a nanotube around its own axis), the E_{1g} mode should be present in cross polarized (ZX) and (XZ) spectra with similar intensities [$I_{A_{1g}(ZZ)}$:$I_{E_{1g}(ZX)}$:$I_{E_{1g}(XZ)}$ = 1.00:0.30:0.30]. Our experimental spectra show a similarity between the (ZX) and (XZ) spectra, but having lower intensity if compared with the intensity in the (ZZ) polarized spectra [$I_{(ZZ)}$:$I_{(ZX)}$:$I_{(XZ)} \sim$ 1.00:0.20:0.20; see Table I].

An interesting result of the observed frequency values is that pairs of peaks at 1549 and 1607 cm^{-1}, or at 1567 and 1590 cm^{-1} are approximately equally shifted from the central graphite frequency ω_g = 1580 cm^{-1}. To explain the frequency shifts of the $E_1(E_{1g})$ and the $E_2(E_{2g})$ modes, Kasuya *et al.* [15] considered that these modes appear at the Γ point of the *nanotube* Brillouin zone as a result of zone folding of the graphene zone. However, their model does not explain the observed splitting ΔA of the $A(A_{1g})$ modes, and their values of ΔE_1 and ΔE_2 for the splittings of the $E_1(E_{1g})$ and the $E_2(E_{2g})$ modes are not in agreement with our observations. According to Kasuya *et al.*, $\Delta E_1 \sim$ 8 cm^{-1} and $\Delta E_2 \sim$ 28 cm^{-1} for d_t = 1.85 nm [15], while we observed ΔE_1 = 23 cm^{-1} and ΔE_2 = 58 cm^{-1}. To account for the observed values for ΔA, ΔE_1, and ΔE_2, it is necessary to consider that the frequency shifts relative to the graphite value ω_g depend also on the nanotube curvature.

Different force constants are expected for vibrations along the nanotube axis relative to the circumferential direction. This curvature effect is responsible for the observed ΔA = 23 cm^{-1} separation between the two $A(A_{1g})$ components at 1567 cm^{-1} (attributed to vibrations in the circumferential direction) and at 1590 cm^{-1} (for vibrations along the nanotube axis). MWNTs are composed of

large diameter tubes ($d_t \sim 25$ nm). Their G-band spectra also exhibit two bands, but these are separated by a smaller amount (9 cm^{-1}) because their curvature effect is smaller [8]. For the $E_2(E_{2g})$ modes in SWNTs, the observed frequency difference $\Delta E_2 = 58$ cm^{-1} between the two $E_2(E_{2g})$ components can be explained qualitatively by taking into account both the frequency differences arising from the curvature effect ($\sim$23 cm^{-1}) and the zone folding effect ($\sim$28 cm^{-1} for $d_t = 1.85$ nm [15]). In the case of the $E_1(E_{1g})$ modes, the observed frequency difference $\omega_{A(A_{1g})} - \omega_{E_1(E_{1g})}$ between the two up-shifted components or between the two down-shifted components is not large enough to be resolved experimentally, which is in part due to inhomogeneous broadening of the $A(A_{1g})$ and $E_1(E_{1g})$ modes related to a diameter dependent distribution of mode frequencies. Our experimental results indicate a much smaller shift due to zone folding for the $E_1(E_{1g})$ modes relative to the $E_2(E_{2g})$ modes, in agreement with Kasuya *et al.* [15]. Though zone folding and curvature effects are both important, further experimental and theoretical work is needed to clarify their relative roles.

Furthermore, some authors have identified a clear dependence of the $E_2(E_{2g})$ mode frequencies on nanotube chirality [2,6,7]. From group theory, all tubes (zigzag, armchair, and chiral) have two $E_2(E_{2g})$ modes. In the case of chiral tubes, both of the E_2 modes are Raman active [6,13], but the Raman cross section is dependent on chiral angle: the lower frequency E_2 mode has a higher intensity for low chiral angle tubes, while the higher frequency E_2 mode has a higher intensity for high chiral angle tubes [13]. For zigzag tubes, only the lower frequency E_{2g} mode is Raman active, while for armchair tubes, only the higher frequency E_{2g} mode is Raman active, as already reported [2,6,7]. We thus identify the 1549 cm^{-1} peak as coming mostly from nanotubes with smaller chiral angles (nearer $\theta = 0°$), and the 1607 cm^{-1} peak as coming mostly from tubes with larger θ (closer to $\theta = 30°$). For a more reliable assignment of the chiral angle dependence of the $A(A_{1g})$ and $E_1(E_{1g})$ mode frequencies, however, more accurate calculations considering the presence of six Raman components and the nanotube curvature effect are needed.

In summary, we have identified the symmetry and the dependence on nanotube geometry of the G-band modes of *semiconducting* SWNTs. The relative Raman intensity of the G-band modes of *semiconducting* SWNT bundles can be basically explained by symmetry considerations for a (10,10) nanotube. The observed discrepancies are related to the presence of different chiral tubes, which require further theoretical and experimental work.

We thank Dr. S. D. M. Brown of MIT for valuable discussions. A. J. acknowledges financial support from CNPq–Brazil. Experimental work was performed at UFMG–Brazil, supported by FAPEMIG, CAPES, and FINEP. A. M. R. thanks MRSEC NSF DMR 98-09686 for support. R. S. thanks Grant-in-Aid (No. 11165216) from the Ministry of Education, Japan. IMR authors thank NSFC Grant No. 59872045. MIT authors acknowledge NSF DMR 98-04734 and No. NSF-INT 98-15744.

*Present address: Department of Physics and Astronomy, Clemson University, Clemson, South Carolina 29634.

[1] R. Saito, G. Dresselhaus, and M. S. Dresselhaus, *Physical Properties of Carbon Nanotubes* (Imperial College Press, London, 1998); M. S. Dresselhaus and P. C. Eklund, Adv. Phys. **49**, 705 (2000).

[2] A. M. Rao, E. Richter, S. Bandow, B. Chase, P. C. Eklund, K. W. Williams, M. Menon, K. R. Subbaswamy, A. Thess, R. E. Smalley, G. Dresselhaus, and M. S. Dresselhaus, Science **275**, 187 (1997).

[3] S. Bandow, S. Asaka, Y. Saito, A. M. Rao, L. Grigorian, E. Richter, and P. C. Eklund, Phys. Rev. Lett. **80**, 3779 (1998); M. Milnera, J. Kürti, M. Hulman, and H. Kuzmany, Phys. Rev. Lett. **84**, 1324 (2000).

[4] M. A. Pimenta, A. Marucci, S. Empedocles, M. Bawendi, E. B. Hanlon, A. M. Rao, P. C. Eklund, R. E. Smalley, G. Dresselhaus, and M. S. Dresselhaus, Phys. Rev. B **58**, R16 016 (1998); M. A. Pimenta, A. Marucci, S. D. M. Brown, M. J. Matthews, A. M. Rao, P. C. Eklund, R. E. Smalley, G. Dresselhaus, and M. S. Dresselhaus, J. Mater. Res. **13**, 2396 (1998); S. D. M. Brown, P. Corio, A. Marucci, M. S. Dresselhaus, M. A. Pimenta, and K. Kneipp, Phys. Rev. B **61**, R5137 (2000); G. S. Duesberg, W. J. Blau, H. J. Byrne, J. Muster, M. Burghard, and S. Roth, Chem. Phys. Lett. **310**, 8 (1999).

[5] H. D. Sun, Z. K. Tang, J. Chen, and G. Li, Solid State Commun. **109**, 365 (1999).

[6] D. Kahn and J. P. Lu, Phys. Rev. B **60**, 6535 (1999).

[7] R. Saito, T. Takeya, T. Kimura, G. Dresselhaus, and M. S. Dresselhaus, Phys. Rev. B **57**, 4145 (1998).

[8] A. M. Rao, A. Jorio, M. A. Pimenta, M. S. S. Dantas, R. Saito, G. Dresselhaus, and M. S. Dresselhaus, Phys. Rev. Lett. **84**, 1820 (2000).

[9] C. Thomsen, S. Reich, P. M. Rafailov, and H. Jantoljak, Phys. Status Solidi (b) **214**, R15 (1999).

[10] H. Kataura, Y. Kumazawa, Y. Maniwa, I. Umezu, S. Suzuki, Y. Ohtsuka, and Y. Achiba, Synth. Met. **103**, 2555 (1999); S. D. M. Brown, A. Jorio, R. Saito, P. Corio, M. S. Dresselhaus, G. Dresselhaus, and K. Kneipp (unpublished).

[11] C. Liu, H. T. Cong, F. Li, P. H. Tan, H. M. Cheng, K. Lu, and B. L. Zhou, Carbon **37**, 1865 (1999).

[12] U. D. Venkateswaran, A. M. Rao, E. Richter, M. Menon, A. Rinzler, R. E. Smalley, and P. C. Eklund, Phys. Rev. B **59**, 10 928 (1999).

[13] R. Saito, A. Jorio, J. Hafner, C. M. Lieber, G. Dresselhaus, and M. S. Dresselhaus (unpublished).

[14] H. Ajiki and T. Ando, Physica (Amsterdam) **201B**, 349 (1994).

[15] A. Kasuya, Y. Sasaki, Y. Saito, K. Tohji, and Y. Nishina, Phys. Rev. Lett. **78**, 4434 (1997).